HUNTINGTON'S DISEASE

Evaluation of mutant huntingtin and neurofilament proteins as potential markers in Huntington's disease

Lauren M. Byrne[1]*†, Filipe B. Rodrigues[1†], Eileanor B. Johnson[1], Peter A. Wijeratne[2], Enrico De Vita[3,4], Daniel C. Alexander[2,5], Giuseppe Palermo[6], Christian Czech[6], Scott Schobel[6], Rachael I. Scahill[1], Amanda Heslegrave[7], Henrik Zetterberg[7,8,9,10], Edward J. Wild[1]*

Huntington's disease (HD) is a genetic progressive neurodegenerative disorder, caused by a mutation in the *HTT* gene, for which there is currently no cure. The identification of sensitive indicators of disease progression and therapeutic outcome could help the development of effective strategies for treating HD. We assessed mutant huntingtin (mHTT) and neurofilament light (NfL) protein concentrations in cerebrospinal fluid (CSF) and blood in parallel with clinical evaluation and magnetic resonance imaging in premanifest and manifest HD mutation carriers. Among HD mutation carriers, NfL concentrations in plasma and CSF correlated with all nonbiofluid measures more closely than did CSF mHTT concentration. Longitudinal analysis over 4 to 8 weeks showed that CSF mHTT, CSF NfL, and plasma NfL concentrations were highly stable within individuals. In our cohort, concentration of CSF mHTT accurately distinguished between controls and HD mutation carriers, whereas NfL concentration, in both CSF and plasma, was able to segregate premanifest from manifest HD. In silico modeling indicated that mHTT and NfL concentrations in biofluids might be among the earliest detectable alterations in HD, and sample size prediction suggested that low participant numbers would be needed to incorporate these measures into clinical trials. These findings provide evidence that biofluid concentrations of mHTT and NfL have potential for early and sensitive detection of alterations in HD and could be integrated into both clinical trials and the clinic.

INTRODUCTION

Huntington's disease (HD) is a progressive, autosomal dominant neurodegenerative disorder characterized by motor, psychiatric, and cognitive dysfunction, caused by CAG expansions in the *HTT* gene, encoding the causative agent, mutant huntingtin (mHTT) (*1*). With multiple targeted "huntingtin-lowering" therapies in clinical development (*2*, *3*), there is a pressing need for sensitive biomarkers of progression and target engagement. If a disease-modifying treatment is developed, there will be an immediate need for tools to aid stratification of premanifest mutation carriers for preventative trials and to guide clinical treatment decisions. However, current clinical assessments and rating scales will be limited for these purposes because they are designed to clinically characterize individuals who have already manifested motor abnormalities (*4*–*8*). Through longitudinal observational studies, robust clinical, cognitive, and structural neuroimaging biomarkers of HD progression have emerged (*9*–*11*). Establishing useful biochemical markers has proven more challenging (*12*).

Quantification of mHTT within the central nervous system (CNS) was reported by Wild and colleagues in 2015, using a novel single-molecule counting immunoassay (*13*). mHTT concentration in the cerebrospinal fluid (CSF) was associated with clinical severity, independently of known predictors, namely age and *HTT* CAG repeat length. CSF mHTT concentration was used to demonstrate successful huntingtin lowering in the first phase 1/2 clinical trial of a huntingtin-lowering therapy, the intrathecally administered antisense oligonucleotide HTT_{Rx}/RG6042 (NCT02519036) (*3*, *14*). A technical validation of this assay was recently published (*15*), but the behavior of CSF mHTT in terms of clinical sensitivity, specificity, and intraindividual stability over time—important characteristics for designing adequately powered biomarker-supported clinical trials—has not been assessed in a clinical cohort.

Neurofilament light protein (NfL) is the smallest subunit of neurofilaments and a component of the neuronal cytoskeleton (*16*). Its release into CSF occurs as a result of neuronal damage (*17*); several studies have shown that NfL is increased in CSF in HD patients and correlates with clinical severity (*18*–*21*). We recently reported, in a retrospective study, the potential of NfL, measured in blood using an ultrasensitive assay, as a prognostic biomarker for HD (*22*). Baseline plasma NfL predicted numerous aspects of subsequent disease course, including rates of brain atrophy, cognitive decline, and disease onset in premanifest HD mutation carriers (preHD). There was a strong correlation between plasma and CSF NfL concentration, implying CNS origin of NfL detected in plasma (*22*). Subsequently, we showed that NfL in plasma predicts regional atrophy in disease-associated brain areas (*23*) and that NfL in CSF and blood is a potential translational biomarker in at least one mouse model of HD (*24*). However, our understanding of the potential value of NfL as a biomarker is limited by the lack of a large, well-phenotyped cohort in which to study it in both plasma and CSF.

These two proteins—mHTT as the pathogenic agent and a pharmacodynamic marker of huntingtin-lowering effect and NfL as a

[1]Huntington's Disease Centre, University College London (UCL) Institute of Neurology, London WC1N 3BG, UK. [2]Centre for Medical Image Computing, Department of Computer Science, UCL, London WC1E 6EA, UK. [3]Lysholm Department of Neuroradiology, National Hospital for Neurology and Neurosurgery, London WC1N 3BG, UK. [4]Department of Biomedical Engineering, School of Biomedical Engineering and Imaging Sciences, King's College London, London SE1 7EH, UK. [5]Clinical Imaging Research Centre, National University of Singapore, Singapore 117599, Singapore. [6]Neuroscience, Ophthalmology, and Rare Diseases, Roche Pharma Research and Early Development, Roche Innovation Center Basel, F. Hoffman–La Roche Ltd., 4070 Basel, Switzerland. [7]Department of Molecular Neuroscience, UCL Institute of Neurology, Queen Square, London WC1N 3BG, UK. [8]UK Dementia Research Institute at UCL, London WC1E 6BT, UK. [9]Department of Psychiatry and Neurochemistry, Institute of Neuroscience and Physiology, Sahlgrenska Academy at the University of Gothenburg, Mölndal, 405 30 Gothenburg, Sweden. [10]Clinical Neurochemistry Laboratory, Sahlgrenska University Hospital, Mölndal, 413 45 Gothenburg, Sweden.
*Corresponding author. Email: lauren.byrne.14@ucl.ac.uk (L.M.B.); e.wild@ucl.ac.uk (E.J.W.)
†These authors contributed equally as first authors.

marker of neuronal damage—have the potential to form a powerful, synergistic biofluid biomarker combination. However, they have never been measured in parallel in CSF and blood from a cohort of HD mutation carriers and controls, accompanied by detailed clinical and magnetic resonance imaging (MRI) data. Assessment of multiple factors in the same individuals should enable the head-to-head evaluation of clinical performances necessary to design appropriate clinical trials. The event-based model (EBM) (*25*) is a data-driven and probabilistic method that computationally models a disease process as a sequence of events in which individual factors become detectably abnormal, as inferred from their distributions in healthy and disease populations. This method has revealed biomarker orderings that provide insight into pathological ordering in Alzheimer's disease (*26*, *27*), multiple sclerosis (*28*, *29*), and, recently, HD (*30*). However, studies in HD investigating the temporal order in which biofluid markers alter during the disease course relative to more established clinical and MRI measures are lacking.

The study presented here, called the HD-CSF study, was designed to generate a resource of CSF matched with blood plasma, along with phenotypic and neuroimaging data, to facilitate HD biofluid biomarker development. Procedures were designed to maximize consistency of data and sample acquisition and processing.

Using baseline samples and data from the HD-CSF cohort, we assessed mHTT in CSF and NfL in CSF and plasma, comparing all three head-to-head against clinical and neuroimaging outcome measures using partial correlations, and their relative diagnostic ability using receiver operating characteristic (ROC) analysis. In a subset of volunteers who underwent a second biosample collection 6 weeks later, we evaluated intraindividual stability of mHTT and NfL. We calculated sample size requirements for clinical trials using reductions in mHTT or NfL as outcome measures. Finally, the temporal sequence in which the measured variables become abnormal was assessed using event-based modeling, providing new insights into the earliest disease-related changes detectable in HD.

RESULTS

The HD-CSF cohort is well matched across disease groups except for age

The HD-CSF cohort consists of 80 participants: 20 healthy controls, 20 preHD, and 40 manifest HD mutation carriers (manifest HD) ranging from early- to moderate-stage HD [Unified HD Rating Scale (UHDRS) total functional capacity, 4 to 13 inclusive). Demographics and baseline characteristics are presented in table S1.

The preHD group was significantly younger than the control and manifest HD groups ($P = 0.012$ and $P < 0.0001$, respectively; table S1), a consequence of their selection as individuals too young to have developed HD symptoms; the control group was recruited to match the mean age of all HD mutation carriers ($P = 0.061$). Therefore, age adjustment was included in all analyses. There were no intergroup differences in gender. As expected, there were no differences between the control and preHD groups for functional, motor, and cognitive scores, but there were differences between the preHD and manifest HD groups (table S1).

In all 80 participants, mHTT concentration was quantified in CSF, whereas NfL concentration was measured in CSF and plasma. Analyte concentrations by group are shown in Table 1. CSF mHTT concentration was quantifiable in all HD mutation carriers but was below the detection threshold in all controls. Thus, controls were excluded from the analysis of confounding variables for mHTT.

We assessed potential confounding variables for each analyte (fig. S1). All three were associated with age (fig. S1, A to C); there was no evidence for an effect of gender on any analyte (fig. S1, D to F). Only CSF mHTT concentrations were associated directly with the number of CAG repeats (fig. S1, G to I); CSF hemoglobin concentration, used to evaluate any effect of blood contamination, was not associated with any analyte (fig. S1, J to L). Nonetheless, because CAG repeat length is the primary driver of HD progression, we repeated all subsequent analyses between the three analytes with other measured variables to include age and CAG repeat length as covariates (Tables 1 and 2). This permits assessment of whether each analyte has independent power to predict cross-sectional disease characteristics, beyond the known best predictors of progression.

mHTT and NfL are higher in manifest HD than controls and preHD, beyond the effects of age and CAG

Consistent with previous reports, the concentrations of CSF mHTT, CSF NfL, and plasma NfL were all significantly higher in HD mutation carriers compared to controls (CSF mHTT, $P < 0.0001$; CSF NfL, $P < 0.0001$; plasma NfL, $P < 0.0001$; Table 1). Each analyte concentration was significantly higher in manifest than preHD (CSF mHTT, $P = 0.001$; CSF NfL, $P < 0.0001$; plasma NfL, $P < 0.0001$;

Table 1. Comparison of analyte concentrations. Intergroup differences were assessed using multiple linear regressions, which included either age or age and CAG as covariates. Significant differences are in bold. *P* values are Bonferroni-corrected. NfL concentrations were natural log–transformed. Values are means ± SD. CAG, CAG repeat length; ANOVA, analysis of variance; N/A, not applicable.

Analyte	Control (*n* = 20)	PreHD (*n* = 20)	Manifest HD (*n* = 40)	Comparison *P* values				
				Adjusted for	Control versus all mutation carriers	ANOVA	Control versus PreHD	PreHD versus manifest HD
CSF mHTT (fM)	0 ± 0	46.4 ± 21.8	73.7 ± 28.7	Age	**<0.0001**	**<0.0001**	**<0.0001**	**0.0010**
				Age and CAG	N/A	N/A	N/A	0.1520
CSF NfL (log pg/ml)	6.7 ± 0.5	7.5 ± 0.7	8.5 ± 0.4	Age	**<0.0001**	**<0.0001**	**<0.0001**	**<0.0001**
				Age and CAG	N/A	N/A	N/A	**0.0148**
Plasma NfL (log pg/ml)	2.9 ± 0.4	3.3 ± 0.6	4.2 ± 0.4	Age	**<0.0001**	**<0.0001**	**<0.0001**	**<0.0001**
				Age and CAG	N/A	N/A	N/A	**0.0008**

Table 2. Association between the analytes and all assessed measures in HD mutation carriers. Values are Pearson's *r* generated by partial correlations including age, or age and CAG, as covariates. Significant associations highlighted in bold. Volumetric measures are percentage of total intracranial volume (TIV).

Clinical measures (*n* = 60)	Adjusted for	CSF mHTT		CSF NfL		Plasma NfL	
		r	*P* value	*r*	*P* value	*r*	*P* value
Total functional capacity	Age	−0.354	**0.0060**	−0.358	**0.0054**	−0.512	**<0.0001**
	Age and CAG	−0.122	0.3618	−0.038	0.7785	−0.291	**0.0267**
Total motor score	Age	0.444	**0.0004**	0.533	**<0.0001**	0.695	**<0.0001**
	Age and CAG	0.208	0.1181	0.249	0.0594	0.525	**<0.0001**
Symbol digit modalities test	Age	−0.333	**0.0108**	−0.463	**0.0003**	−0.562	**<0.0001**
	Age and CAG	−0.061	0.6551	−0.140	0.2985	−0.329	**0.0125**
Stroop color naming	Age	−0.351	**0.0064**	−0.509	**<0.0001**	−0.650	**<0.0001**
	Age and CAG	−0.072	0.5931	−0.208	0.1166	−0.454	**0.0003**
Stroop word reading	Age	−0.388	**0.0024**	−0.528	**<0.0001**	−0.702	**<0.0001**
	Age and CAG	−0.108	0.4178	−0.219	0.0989	−0.525	**<0.0001**
Verbal fluency categorical	Age	−0.370	**0.0040**	−0.445	**0.0004**	−0.577	**<0.0001**
	Age and CAG	−0.097	0.4672	−0.103	0.4401	−0.340	**0.0091**
Imaging measures (*n* = 49)							
Whole-brain volume	Age	−0.234	0.1102	−0.479	**0.0006**	−0.406	**0.0042**
	Age and CAG	−0.082	0.5862	−0.452	**0.0014**	−0.285	0.0518
White matter volume	Age	−0.142	0.3360	−0.354	**0.0135**	−0.205	0.1626
	Age and CAG	−0.053	0.7246	−0.351	**0.0157**	−0.122	0.4150
Gray matter volume	Age	−0.266	0.0674	−0.507	**0.0002**	−0.477	**0.0006**
	Age and CAG	−0.151	0.3116	−0.398	**0.0057**	−0.404	**0.0049**
Caudate volume	Age	−0.211	0.1547	−0.539	**0.0001**	−0.718	**<0.0001**
	Age and CAG	−0.025	0.8682	−0.358	**0.0144**	−0.628	**<0.0001**

after Bonferroni correction for multiple comparisons; Table 1 and Fig. 1, A to C). The concentration of the three analytes was also higher in preHD than in healthy controls (CSF mHTT, $P = 0.001$; CSF NfL, $P < 0.0001$; plasma NfL, $P < 0.0001$; after Bonferroni correction; Table 1 and Fig. 1, A to C). The manifest HD group had significantly increased concentrations of CSF NfL and plasma NfL compared with the preHD group after adjustment for age and CAG, also surviving multiplicity correction (CSF NfL, $P = 0.0148$; plasma NfL, $P = 0.0008$; Table 1).

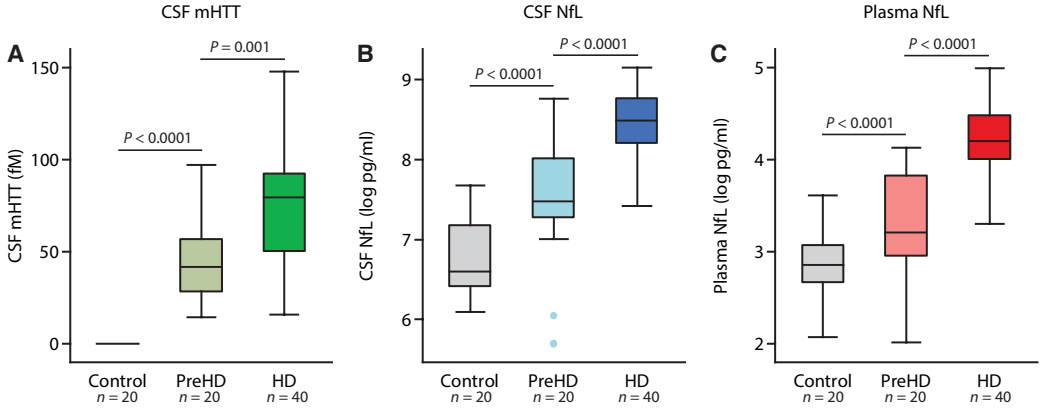

Fig. 1. Comparison of analyte concentrations across disease stage. Concentration of (**A**) CSF mHTT, (**B**) CSF NfL, and (**C**) plasma NfL in healthy controls, PreHD, and manifest HD (HD) patients. NfL values are natural log–transformed. *P* values were generated from multiple linear regressions and are Bonferroni-corrected.

Plasma NfL has the strongest association with clinical severity compared to CSF NfL and mHTT

Among HD mutation carriers, there were statistically significant associations, after age adjustment, between CSF mHTT, CSF NfL, and plasma NfL concentrations and all prespecified UHDRS clinical measures: total functional capacity (Table 2 and Fig. 2, A to C), total motor score (Table 2 and Fig. 2, D to F), symbol digit modalities test (Table 2 and Fig. 2, G to I), Stroop color naming (Table 2), Stroop word reading (Table 2 and Fig. 2, J to L), and verbal fluency categorical (Table 2). Only the associations between plasma NfL and the clinical measures remained when the results were adjusted for the number of CAG repeats in addition to age (Table 2).

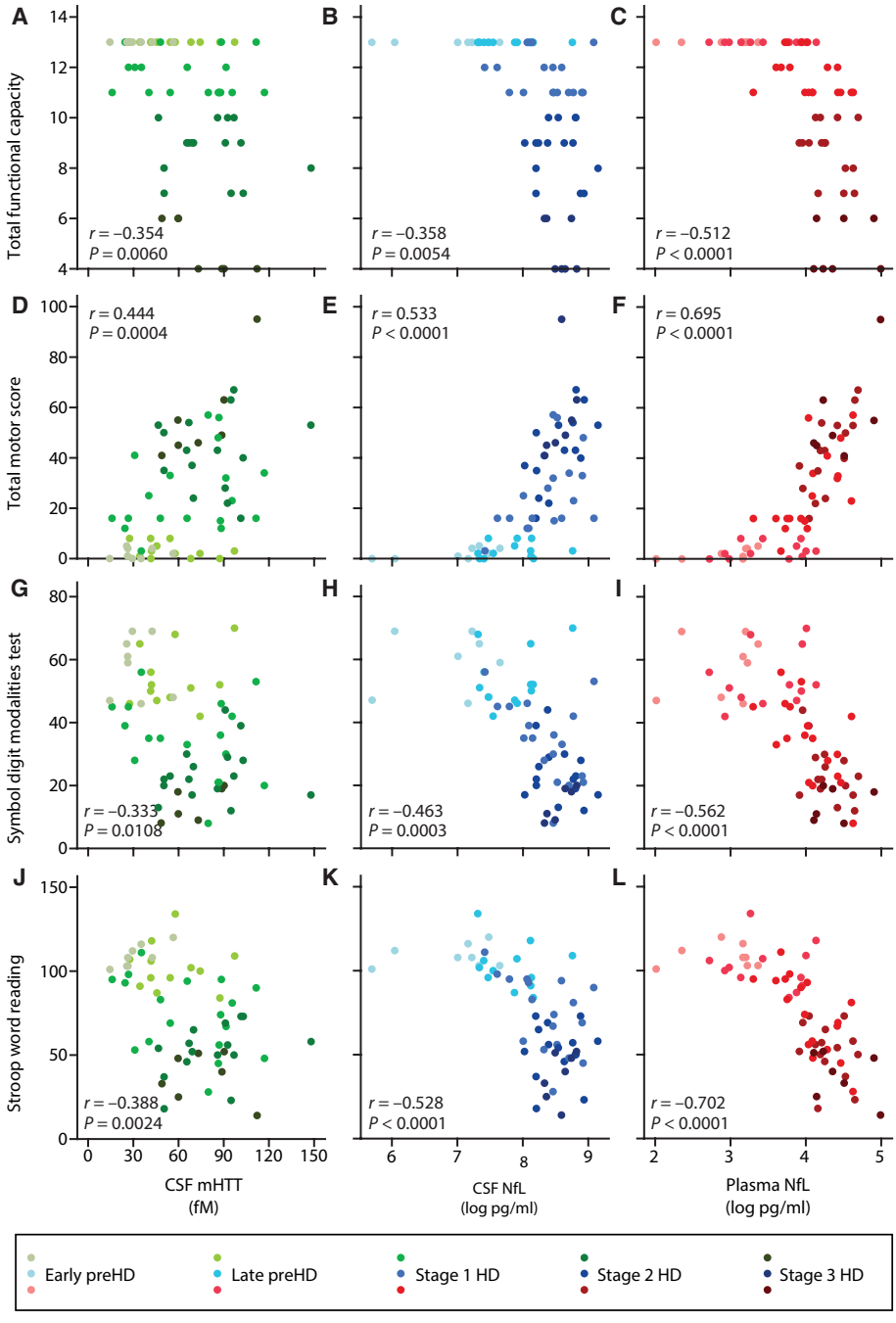

Fig. 2. Comparison of analyte concentrations and clinical measures. Association within HD mutation carriers ($n = 60$) between CSF mHTT (green; **A**, **D**, **G**, and **J**), CSF NfL (blue; **B**, **E**, **H**, and **K**), plasma NfL (red; **C**, **F**, **I**, and **L**), and UHDRS clinical scores including functional (A to C), motor (D to F), and cognitive (G to L) measures. Scatter plots show unadjusted values. *r* and *P* values are age-adjusted, generated from Pearson's partial correlations including age as a covariate. NfL values are natural log–transformed.

CSF NfL predicts brain volume more closely than plasma NfL or CSF mHTT

Sixty-four participants (80%) had an MRI scan, of whom 49 were HD mutation carriers. Their demographic, clinical, and biochemical characteristics were similar to those who did not have MRI scans (table S2). CSF mHTT concentration was not associated with brain volume (Table 2 and Fig. 3, A to D). CSF NfL concentration was associated with every prespecified MRI volume measurement: whole brain (Table 2 and Fig. 3E), white matter (Table 2 and Fig. 3F), gray matter (Table 2 and Fig. 3G), and caudate (Table 2 and Fig. 3H), all calculated as a percentage of TIV and age-adjusted. These associations survived additional adjustment for age and number of CAG repeats (Table 2). Plasma NfL concentration was associated with whole brain (Table 2 and Fig. 3I), gray matter (Table 2 and Fig. 3K), and caudate volumes (Table 2 and Fig. 3L); the associations with gray matter and caudate survived adjustment for age and CAG (Table 2).

CSF NfL and plasma NfL are more closely correlated than CSF NfL and mHTT

In HD mutation carriers, concentrations of mHTT and NfL in CSF were strongly correlated (unadjusted, $r = 0.682$, $P < 0.0001$; age-adjusted, $r = 0.697$, $P < 0.0001$; Fig. 4A). In the whole cohort, CSF and plasma NfL were also highly correlated (unadjusted, $r = 0.914$, $P < 0.0001$; age-adjusted, $r = 0.885$, $P < 0.0001$; Fig. 4B). In HD mutation carriers, the correlation persisted (unadjusted, $r = 0.878$, $P < 0.0001$; age-adjusted, $r = 0.794$, $P < 0.0001$; Fig. 4B). The mean concentration of NfL in CSF for all participants was 33.7 times that in plasma. HD mutation carriers had a significantly higher CSF/plasma ratio for NfL than controls (36.5 and 25.5, respectively; $P = 0.0010$), consistent with our previous findings in a smaller cohort (*9*).

CSF mHTT, CSF NfL, and plasma NfL have favorable attributes for clinical application

We analyzed the sensitivity and specificity of each analyte by examining its ability to discriminate between HD mutation carriers and controls and between manifest and preHD, using ROC curves, in which the true-positive rate (sensitivity) is plotted against the false-positive rate (1 – specificity) for each analyte value. The area under a ROC curve (AUC) gives a measure of a test's accuracy (that is, its discriminatory ability); 0.5 indicates a 50% probability of the test giving the correct answer, whereas 1 indicates a test that gives the correct answer every time (*31*).

For distinguishing between controls and HD mutation carriers, CSF mHTT had essentially perfect accuracy (AUC, 1.000; Fig. 5A). CSF and plasma NfL both displayed high accuracy [AUC, 0.933 (CSF) and 0.914 (plasma); Fig. 5A]. The accuracy of NfL was not statistically significantly different between CSF and plasma ($P = 0.364$).

For distinguishing between preHD and manifest HD, mHTT displayed moderate accuracy (AUC, 0.775; Fig. 5B). NfL, however, had high accuracy in both CSF and plasma [AUC, 0.914 (CSF) and 0.931 (plasma); Fig. 5B]. The accuracy of NfL was not statistically significantly

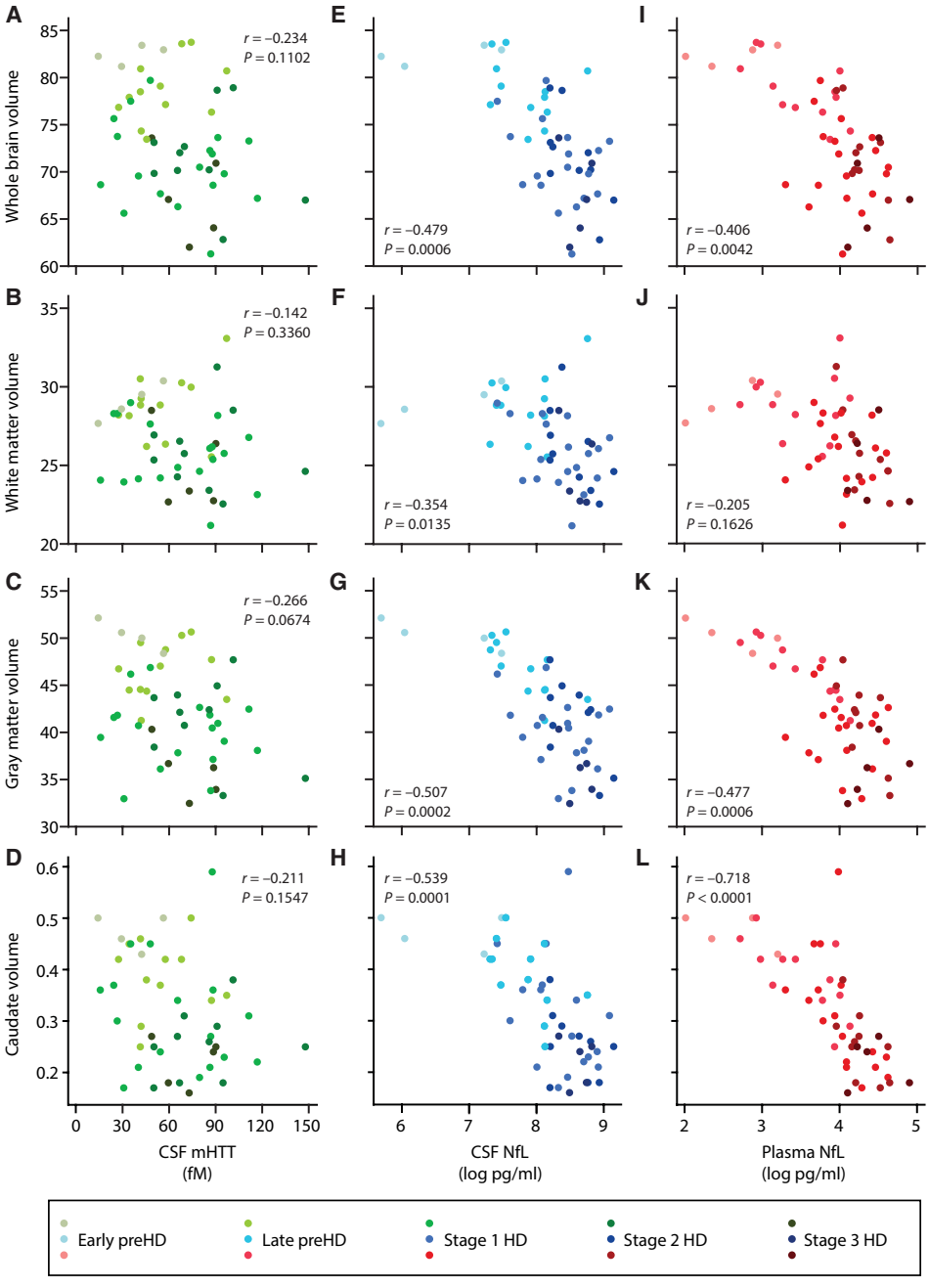

Fig. 3. Comparison of analyte concentrations and imaging measures. Association within HD mutation carriers ($n = 49$) between the analytes CSF mHTT (green; **A** to **D**), CSF NfL (blue; **E** to **H**), plasma NfL (red; **I** to **L**), and MRI volumetric measures of whole brain (A, E, and I), white matter (B, F, and J), gray matter (C, G, and K), and caudate (D, H, and L). All volumetric measures were calculated as a percentage of TIV. Scatter plots show unadjusted values. *r* and *P* values are age-adjusted, generated from Pearson's partial correlations including age as a covariate. NfL values are natural log–transformed.

different between CSF and plasma ($P = 0.5800$), but each was significantly superior to that of CSF mHTT (CSF NfL, $P = 0.0039$; plasma NfL, $P = 0.0125$).

To assess intraindividual stability of each analyte, 15 participants (18.8%) underwent a second sampling visit 4 to 8 weeks after the first (mean interval, 39.1 days), where CSF and blood were collected under the same conditions. This group comprised 2 controls, 3 preHD, and 10 manifest HD. Their demographic, clinical, and biochemical characteristics were similar to those who declined repeat sampling (table S3). The intraclass correlation between the first and second sampling visits in this cohort was high for all analytes [CSF mHTT, 0.937 (95% CI, 0.83 to 0.98); Fig. 5C; CSF NfL, 0.995 (95% CI, 0.99 to 1.00); Fig. 5D; plasma NfL, 0.954 (95% CI, 0.87 to 0.98); Fig. 5E].

To inform the design of clinical trials, we performed sample size calculations using the repeated measure data to infer intersubject variability in change from baseline to 6 weeks and assuming null mean change from baseline to 6 weeks in a placebo group. Figure 5F shows the sample sizes required per arm, for theoretical trials in HD mutation carriers for a range of treatment effect sizes. The sample sizes are substantially smaller than those that would likely be required for the clinical endpoints of such trials (*32*).

mHTT and NfL are among the earliest changes detectable in HD

EBM analysis (*30*) applied to the HD-CSF cohort, incorporating all measures of interest, placed CSF mHTT as the earliest detectable change, followed by plasma and CSF NfL (Fig. 6, A and B). The subsequent changes were caudate volume, total motor score, global brain volumes, Stroop color naming, symbol digit modalities test, Stroop word reading, and verbal fluency categorical. The model generated from EBM can be assessed by its ability to stage participants on the basis of their individual data for all measured variables combined; this model accurately characterized all control participants into stage 0, all preHD participants into "low-mid" stage, and nearly all manifest HD patients into "mid-late" stages (Fig. 6C). We reproduced this EBM analysis in the TRACK-HD cohort (*30*) to include plasma NfL, which we previously quantified (*22*). Plasma NfL placed very early in the temporal sequence order—between putamen and caudate volumes (Fig. 6, D and E). Putamen volume was not a prespecified imaging measure in HD-CSF because it is challenging to quantify reliably and performs poorly as a longitudinal measure of progression. Full staging of the adapted TRACK-HD EBM is presented in fig. S2.

DISCUSSION

In this 80-participant cross-sectional study of HD mutation carriers and matched healthy controls—each undergoing rigorously standardized CSF and blood sample collection, phenotypic assessment,

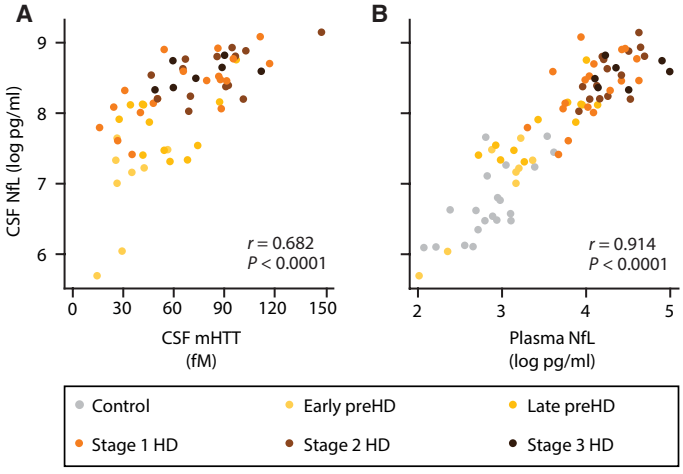

Fig. 4. Associations between biofluid analyte concentrations. Scatter plots showing correlation between CSF mHTT and CSF NfL concentrations (**A**; $n = 60$) and between CSF NfL and plasma NfL (**B**; $n = 80$). Scatter plots show unadjusted values. *r* and *P* values are unadjusted, generated from Pearson's correlations. NfL values were natural log–transformed.

and (in those opting for an optional MRI scan) supporting MRI acquisition—we compared CSF mHTT, CSF NfL, and plasma NfL concentration head-to-head to investigate their relative associations with clinical measures and discriminatory ability. Having corroborated previous findings that these three analytes are associated with measures of disease severity (*13*, *20*, *22*, *33*), we showed that plasma NfL concentration had the strongest associations and independent predictive ability for all clinical measures after adjustment for age and number of CAG repeats. CSF NfL was most strongly associated with all brain volume measures, and these associations remained significant after age and number of CAG repeat adjustment.

All correlations with clinical and imaging measures were stronger for NfL in CSF and plasma than for mHTT in CSF. This perhaps reflects that NfL, as a marker of axonal damage, has a more direct relationship with the development of clinical manifestations and brain atrophy. On the other hand, mHTT may be a less direct predictor of clinical severity. The signal obtained by the CSF mHTT assay is influenced by more than the absolute intraneuronal concentration of mHTT, which likely changes in brain much less than the several-fold changes seen in assay signal in CSF. A higher signal readout is generated by longer polyglutamine length (*15*), reflecting the polyglutamine-dependent binding of MW1 antibody. Somatic instability of the CAG repeat length is increasingly recognized as a potential driver of pathology in HD (*34*, *35*). Further expansion of CAG repeat length in brain tissue, in addition to varying amounts of N-terminal huntingtin fragments and aggregates, may contribute to the relatively large intersubject variability in CSF mHTT concentration as well as its increasing with disease progression. These caveats have little implication for CSF mHTT's utility in huntingtin-lowering trials, which involve quantifying within-subject reductions of mHTT as the pathogenic agent.

The CSF concentrations of mHTT and NfL were closely associated. In turn, NfL concentration was strongly correlated between CSF and plasma, consistent with findings in smaller cohorts examining each association separately (*13*, *22*). This is in keeping with the likely chain of events that links these analytes. mHTT is produced in neurons where it causes damage and ultimately death (*1*, *36*). Some mHTT may be released from damaged or dying neurons and enter the CSF, where it can be measured. This has been shown by the increase in CSF mHTT concentration after experimentally inducing neuronal death in mice expressing mHTT (*33*). The multiple factors contributing to the mHTT assay signal mean that an mHTT-independent measure of neuronal damage might be an important means of establishing the effects of CSF mHTT reduction and might help to dissect which of the three factors (cellular mHTT concentration, somatic instability, or neuronal damage) contribute to the reduction in CSF mHTT signal after a long-term huntingtin-lowering treatment. NfL appears to be a good candidate to serve this purpose. NfL is produced throughout neurons and principally resides in axons. Its concentration rises after insults such as head injury, multiple sclerosis relapses (*37*–*40*), and stroke (*41*), indicating that NfL concentration reflects the current degree of neuronal damage and/or death from different causes. NfL in blood and CSF has been reported to increase within 2 weeks after head trauma (*37*, *42*). Our head-to-head findings suggest that whereas CSF mHTT and plasma NfL both reflect clinical state, CSF NfL was generally more closely associated with measures of brain volume in HD and retained independent associations after adjustment for age and number of CAG repeats, suggesting that it reflects historical brain volume loss beyond other known predictors—age and CAG repeats. This is in keeping with an indicator of neuronal injury progression.

The weaker associations of plasma NfL with global brain volume measures compared to CSF NfL are perhaps unsurprising given that NfL in the periphery is a less direct reflection of neuronal injury. This does not mean that plasma NfL offers no insights into brain atrophy, either historically (brain volume) or prospectively (ongoing brain atrophy). Our previous work suggests that NfL is a dynamic marker of ongoing neuronal damage in HD that predicts subsequent progression (*22*, *23*). The strong association between plasma NfL and caudate volume, even after adjustment for age and number of CAG repeats, corroborates previous findings (*23*) and further demonstrates that plasma NfL has a robust relationship with historical caudate atrophy. The smaller sample size here likely explains the lack of a significant association between plasma NfL and white matter volume, as was seen in the larger TRACK-HD cohort (*23*).

CNS neuronal injury is widely accepted as the source of elevated NfL in blood plasma in neurodegenerative diseases including HD (*22*, *43*–*45*). Although huntingtin-lowering therapeutics currently being tested are administered intrathecally, implying the ready availability of CSF for therapeutic monitoring, orally and intravenously administered therapeutics are under development (*2*) for which a biomarker of neuronal rescue in a readily accessible biofluid would be desirable. Moreover, an accessible biomarker reflecting the current rate of neuronal injury could eventually be useful for guiding clinical decisions, such as when to escalate to more invasive CSF monitoring as a first step toward intrathecal treatment.

Our ROC analysis revealed that there was no significant difference between CSF and plasma NfL in discriminating between disease groups. In its ability to distinguish between controls and mutation carriers, CSF mHTT was unsurprisingly superior to both CSF and plasma NfL, but NfL in either CSF or plasma surpassed mHTT in discriminating between preHD and manifest HD. One important caveat here is that although plasma and CSF NfL appear equivalent in tracking the natural history of HD over years of progression, we do not yet know how quickly either might respond to the rapid

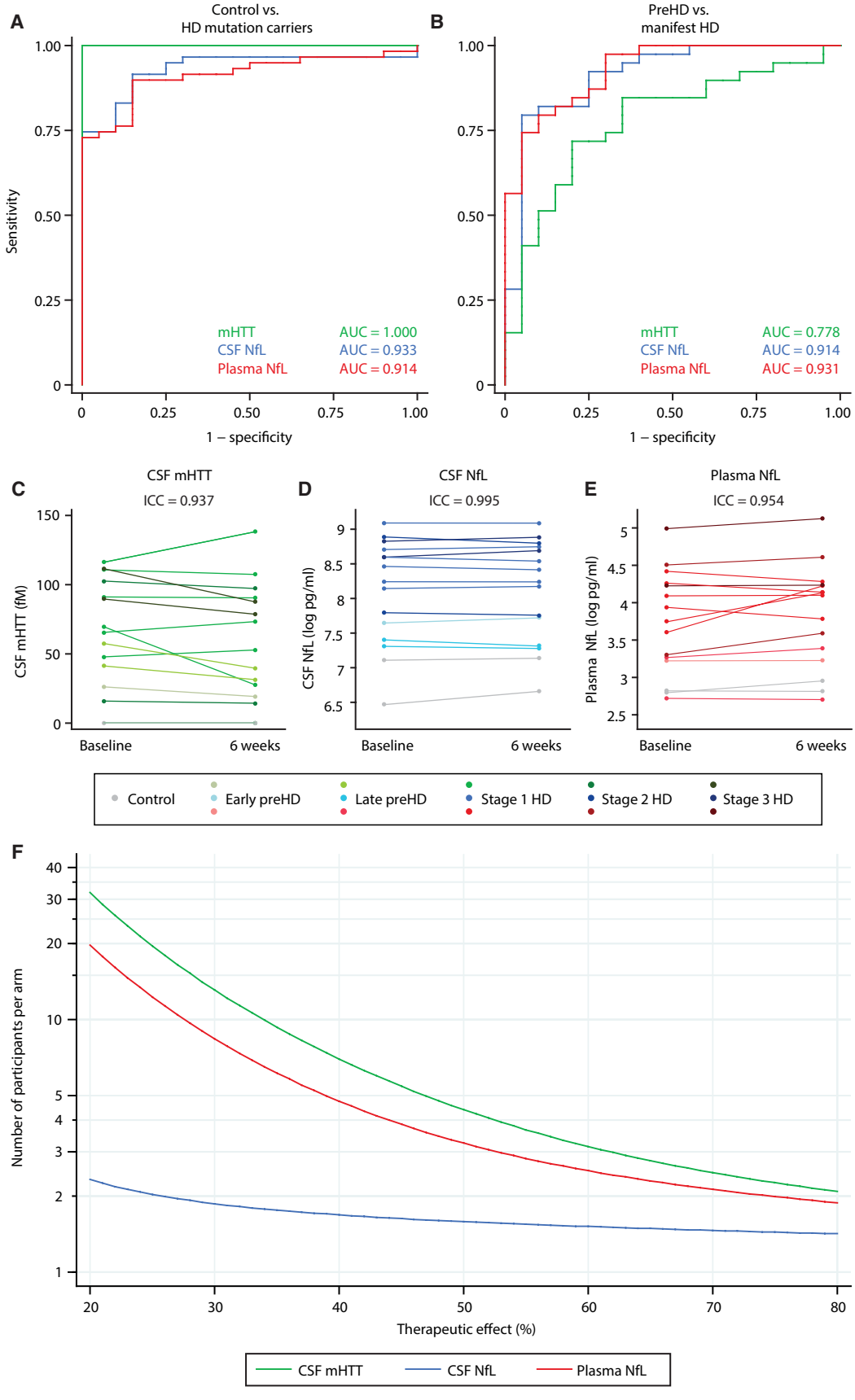

Fig. 5. Parallel assessment of the three analytes on diagnostic ability, within-subject stability, and sample size requirements. (**A** and **B**) ROC curves for (A) discrimination between controls ($n = 20$) and HD mutation carriers [$n = 60$; 95% confidence intervals (CIs) for AUCs: CSF mHTT, 1.000 to 1.000; CSF NfL, 0.876 to 0.989; plasma NfL, 0.852 to 0.976] and (B) discrimination between preHD and manifest HD ($n = 60$; 95% CIs for AUCs: CSF mHTT, 0.650 to 0.900; CSF NfL, 0.831 to 0.996; plasma NfL, 0.869 to 0.993). (**C** to **E**) Stability of CSF mHTT (green; C), CSF NfL (blue; D), and plasma NfL (red; E), over 6 to 8 weeks. Lines linking points indicate samples from the same individual ($n = 15$). (**F**) Sample size calculations for clinical trials in HD mutation carriers, implementing the reduction in these analytes as an outcome measure. NfL values are natural log–transformed. Log-transformed mHTT was used for sample size calculations. ICC, interclass correlation.

amelioration of pathology as may occur with sustained huntingtin lowering. It is likely that any such change would first be reflected in CSF before eventually being apparent in plasma. Serum NfL concentration took 3 months to normalize after a boxing bout (*46*), which may indicate the most rapid reduction in NfL that may be expected if a therapy truly alleviates neuronal pathology.

We investigated CSF in HD patients with longitudinal sampling over 4 to 8 weeks, permitting the intraindividual stability of each analyte to be assessed. The very high intraclass correlation values of the three markers revealed them to be highly stable, suggesting that intraindividual variation in these analytes is likely to be a minimal source of noise in natural history and therapeutic studies.

Our sample size calculations reveal that fewer than 35 participants per group would be sufficient to detect drug-related alterations in HD mutation carriers—whether premanifest or manifest—for all three

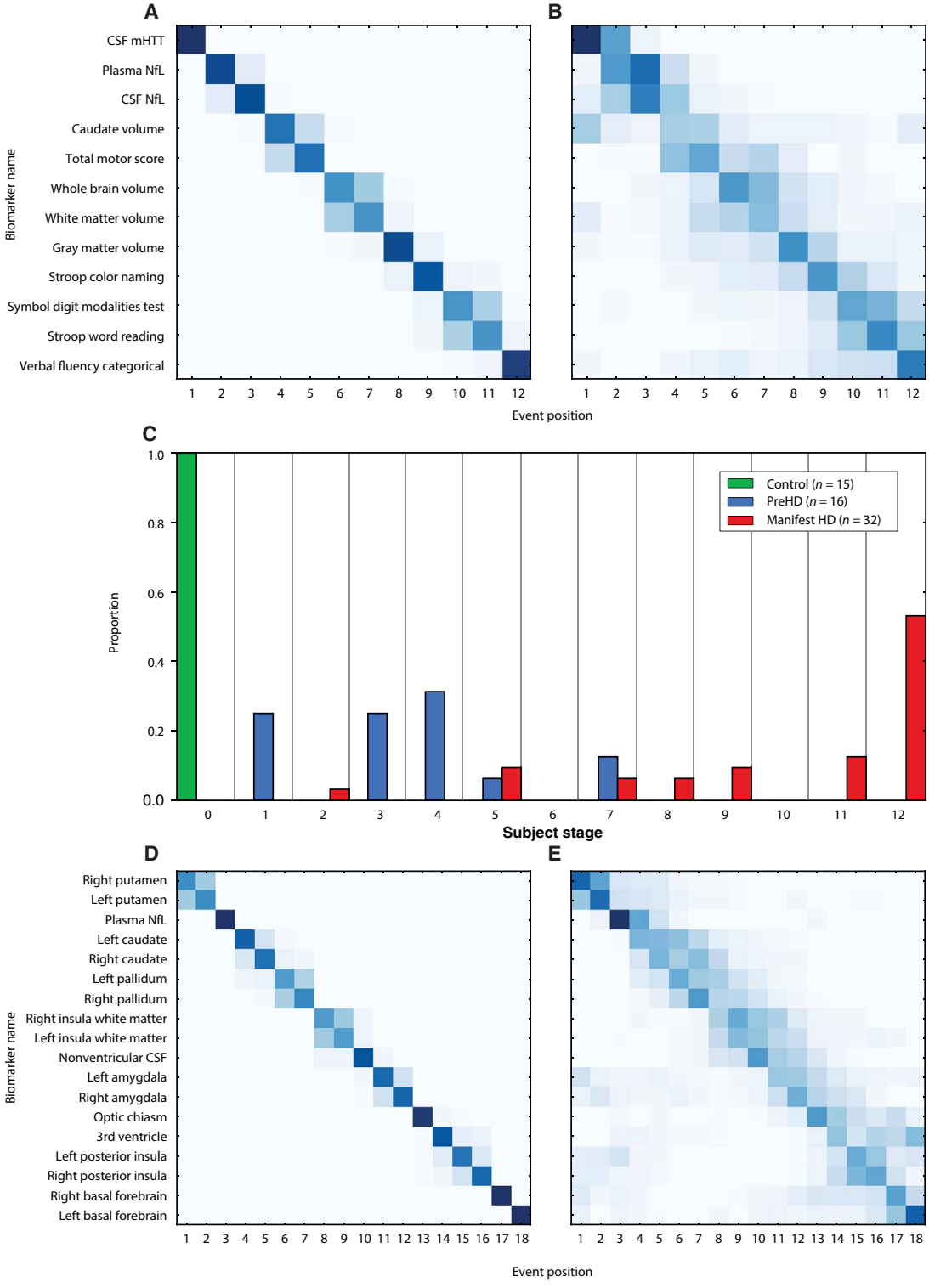

Fig. 6. Comparison of the temporal order of biofluid analytes relative to clinical and imaging measures. (**A**) Positional variance diagram produced from the EBM, applied to the 63 HD-CSF participants who had data for all biomarkers (controls, 15; preHD, 16; manifest HD, 32). (**B**) Reestimation of the positional variance in (A), using 100 bootstrap samples of the data, providing internal validation of the model's findings. (**C**) Distribution of HD-CSF participants staged using the HD-CSF EBM, based on their collective data for all 12 measured variables. (**D**) Positional variance diagram from the EBM using the TRACK-HD cohort (*24*), now including plasma NfL and (**E**) similar results after reestimation with 100 bootstrap samples of the data. The positional variance diagrams represent the sequence of "events" (the individual measures going from normal to abnormal, identified by the EBM). Darker diagonal squares represent higher certainty of the biomarker becoming abnormal at the corresponding event where multiple event boxes colored indicate more uncertainty about its position. 1 indicates the earliest event. Proportion is with respect to each study group.

markers, even at therapeutic effect sizes as low as 20%. This is considerably smaller than the cohort sizes likely to be enrolled in late-phase efficacy trials, indicating that NfL or mHTT quantification could be used to support interim or exploratory analyses without significant sample size cost (*32*, *47*). An important caveat here is that assuming a variability based on within-subject change over 6 weeks may underestimate the variability over the time period of a late-phase efficacy trial.

The MRI-focused EBM analysis of Wijeratne and colleagues in the TRACK-HD cohort (*30*) outlined a fine-grained sequential pattern in brain atrophy, permitting the staging of HD mutation carriers based on brain MRI measures. The HD-CSF cohort permits the exploration of biofluid, imaging, and clinical measures head-to-head. EBM in this cohort suggests that these biofluid analytes—mHTT in CSF and NfL in CSF and plasma—are among the earliest changes detectable in HD. CSF mHTT rose first, then plasma and CSF NfL, which were positionally interchangeable with caudate volume. Next, total motor score and whole brain and white matter volumes changed, followed by gray matter volume and then, finally, the cognitive scores. We were able to further validate these findings for plasma NfL in the larger TRACK-HD cohort, showing that plasma NfL was altered between putamen and caudate atrophy. These findings suggest a potential early role for these biofluid measures in stratifying patients for preventative clinical trials in preHD.

Our study has some limitations that should be acknowledged. First, HD-CSF has relatively small PreHD and control groups because it was designed predominantly as a study of manifest HD. This limits our ability to determine the earliest detection of alterations in both NfL and mHTT as result of the HD gene. Second, longitudinal data over a longer time interval are needed to understand how these analytes vary with disease course and compare head-to-head their ability to predict disease progression. It would also be of interest to perform EBM or similar data-driven models using longitudinal data. Third, our study does not include any individuals with juvenile HD. It will be of interest to understand whether these individuals display similar or different profiles for the variables measured here. Fourth, for application in clinical decision-making, substantial further investigation of the predictive power of NfL in individual patients will be required. Fifth, sampling visits were conducted at around the same time after an overnight fast. We therefore cannot exclude the possibility that these analytes may be affected by diet or time of day. This is worthy of dedicated study. Finally, signals from immunoassays are dependent on the reagents used that may vary between batches or sources. This means that results are most interpretable when used in a single run, within a cohort.

In conclusion, parallel evaluation of CSF mHTT, CSF NfL, and plasma NfL in the HD-CSF cohort revealed that plasma NfL was most strongly associated with measures of clinical severity and that only NfL was associated with MRI brain volume. Through ROC analysis, we showed that NfL has greater clinical discriminatory ability than mHTT, within HD mutation carriers. All analytes were stable over short intervals, and the sample size numbers required for trials of drugs expected to alter these proteins are attainable within the numbers likely required to show clinical efficacy. Finally, we provide evidence through EBM that these biofluid analytes are among the earliest detectable changes as HD progresses. These results suggest that as our understanding grows further, analysis of mHTT and NfL might be useful for developing HD therapeutics and for clinical management.

MATERIALS AND METHODS

Study design

The study aimed to investigate mHTT in CSF, NfL in CSF, and NfL in plasma—and their relative performance as biofluid indicators for HD. Eighty participants (20 healthy controls, 20 preHD, and 40 manifest HD) were recruited from the National Hospital for Neurology and Neurosurgery/University College London/University College London Hospitals HD Multidisciplinary Clinic as part of an ongoing longitudinal, single-site, CSF collection initiative, called HD-CSF. The sample size for the HD-CSF cohort was derived from a priori sample size calculations, based on a 12-subject CSF analysis of mHTT (*13*). Although detecting cross-sectional differences in mHTT concentration between control and HD mutation carriers requires very small numbers (<5 per group for >90% power and two-sided 5% type I error), 20 subjects per group were recruited to allow >90% power for detecting predicted longitudinal change in mHTT over 2 years, imputed from the intergroup differences in mHTT and age in our previous cross-sectional study. Sample collections were standardized as previously reported (*13*, *48*) and described in detail in Supplementary Methods. MRI scans and repeat sampling visits were optional. Clinical and imaging measures of interest were prespecified on the basis of previously published evidence that these measures were most robustly associated with disease progression (*11*, *22*, *49*). Quantification of analytes and MRI processing was performed blinded to disease status. CSF mHTT concentration was measured in triplicate. NfL in CSF and blood was measured in duplicate. Healthy controls were recruited simultaneously and age-matched to HD mutation carriers and were clinically healthy with no evidence of incidental neurological disease.

Data from the multisite TRACK-HD study were used in the EBM analysis. This involved 290 participants of the 366 enrolled at baseline (95 healthy controls, 103 PreHD, and 92 early HD), each of whom had baseline plasma NfL and quality-controlled imaging data.

Structural MRI processing

All T1-weighted scans passed visual quality control check for the presence of significant motion or other artifacts before processing. Bias correction was performed using the N3 procedure (*50*). A semiautomated segmentation procedure via Medical Image Display Analysis Software (MIDAS) was used to generate volumetric regions of the whole brain and TIV, as previously described (*51*–*53*). In addition, SPM12 "Segment" (MATLAB version 2012b) was used to measure the volume of the gray and white matter (*54*). Finally, MALP-EM was used to quantify caudate volume (*55*). MALP-EM is an automated tool used to segment MRI scans into regional volumes and has previously been validated for use in HD cohorts (*56*). Default settings were used for both SPM12 segmentations and MALP-EM caudate regions. No scans failed processing after visual quality control of segmentations by experienced raters to ensure accurate delineation of the regions. Demographic MRI volumes were presented adjusted for TIV. All MRI analyses used brain volumes as percentage of TIV.

Statistics

Analyses were performed with Stata 14.2 (StataCorp). Significance level was defined as $P < 0.05$.

Analyte distributions were tested for normality, and if necessary, arithmetical transformations were evaluated to produce normality. CSF mHTT concentration had a normal distribution. CSF and plasma NfL concentrations were non-normally distributed; a natural logarithm transformation produced an acceptable normal distribution

for both CSF and plasma NfL, as previously shown (*22*); therefore, transformed values were used for all analyses. Unless otherwise specified, outliers were included in the analyses.

Potentially confounding demographic variables (age, gender, and blood contamination) were examined in preliminary analyses; those found to be significant were included as covariates for subsequent analyses. All analyses are reported with the adjustment for potentially confounding demographic variables. All analyses were repeated with adjustment for age and number of CAG repeats—a planned second-level analysis—to assess associations with measures beyond the known combined effect of age and *HTT* CAG repeat length.

We used unpaired two-sample *t* test/ANOVA or the Pearson's χ^2 test to assess intergroup differences of baseline characteristics. Intergroup analyte comparisons were tested using multiple linear regressions using age, or both age and number of CAG repeats, as covariates and were Bonferroni-corrected for multiple comparisons. Correlations were tested using Pearson's correlation and partial correlations for covariate adjustment.

To understand the diagnostic power of the studied analytes, we produced ROC curves for each analyte and compared the AUC formally using the method suggested by DeLong and colleagues (*57*).

We performed sample size calculations to inform the design of therapeutic trials aiming to lower these analytes by a range of desired therapeutic effect sizes. Log-transformed values were used for each analyte. The assumption for intersubject variability was based on the variability in the change from baseline to 6 weeks in HD mutation carriers. No change over time was assumed for the hypothetical control arm of the trial. On the basis of these assumptions, we derived the sample size per arm required to detect a given control-adjusted percent reduction in the treatment arm with 80% power and two-sided 5% type I error.

SUPPLEMENTARY MATERIALS

www.sciencetranslationalmedicine.org/cgi/content/full/10/458/eaat7108/DC1
Methods
Fig. S1. Assessments for potential confounding variables.
Fig. S2. The distribution of TRACK-HD participants staged using EBM.
Fig. S3. The residual distributions for each measure used in the HD-CSF EBM.
Table S1. Baseline characteristics of the HD-CSF cohort.
Table S2. Characteristics of participants who opted out of optional MRI scan.
Table S3. Characteristics of participants who opted out of optional repeated sampling.

REFERENCES AND NOTES

1. C. A. Ross, E. H. Aylward, E. J. Wild, D. R. Langbehn, J. D. Long, J. H. Warner, R. I. Scahill, B. R. Leavitt, J. C. Stout, J. S. Paulsen, R. Reilmann, P. G. Unschuld, A. Wexler, R. L. Margolis, S. J. Tabrizi, Huntington disease: Natural history, biomarkers and prospects for therapeutics. *Nat. Rev. Neurol.* **10**, 204–216 (2014).
2. E. J. Wild, S. J. Tabrizi, Therapies targeting DNA and RNA in Huntington's disease. *Lancet Neurol.* **16**, 837–847 (2017).
3. F. B. Rodrigues, E. J. Wild, Huntington's Disease Clinical Trials Corner: February 2018. *J. Huntingtons. Dis.* **7**, 89–98 (2018).
4. T. A. Mestre, A.-C. Bachoud-Lévi, J. Marinus, J. C. Stout, J. S. Paulsen, P. Como, K. Duff, C. Sampaio, C. G. Goetz, E. Cubo, G. T. Stebbins, P. Martinez-Martin; Members of the MDS Committee on Rating Scales Development, Rating scales for cognition in Huntington's disease: Critique and recommendations. *Mov. Disord.* **33**, 187–195 (2018).
5. T. A. Mestre, M. J. Forjaz, P. Mahlknecht, F. Cardoso, J. J. Ferreira, R. Reilmann, C. Sampaio, C. G. Goetz, E. Cubo, P. Martinez-Martin, G. T. Stebbins, Rating scales for motor symptoms and signs in Huntington's disease: Critique and recommendations. *Mov. Disord. Clin. Pract.* **5**, 111–117 (2018).
6. T. A. Mestre, E. van Duijn, A. M. Davis, A.-C. Bachoud-Lévi, M. Busse, K. E. Anderson, J. J. Ferreira, P. Mahlknecht, V. Tumas, C. Sampaio, C. G. Goetz, E. Cubo, G. T. Stebbins, P. Martinez-Martin; Members of the MDS Committee on Rating Scales Development, Rating scales for behavioral symptoms in Huntington's disease: Critique and recommendations. *Mov. Disord.* **31**, 1466–1478 (2016).
7. T. A. Mestre, M. Busse, A. M. Davis, L. Quinn, F. B. Rodrigues, J.-M. Burgunder, N. E. Carlozzi, F. Walker, A. K. Ho, C. Sampaio, C. G. Goetz, E. Cubo, P. Martinez-Martin, G. T. Stebbins; Members of the MDS Committee on Rating Scales Development, Rating scales and performance-based measures for assessment of functional ability in Huntington's disease: Critique and recommendations. *Mov. Disord. Clin. Pract.* **5**, 361–372 (2018).
8. T. A. Mestre, N. E. Carlozzi, A. K. Ho, J.-M. Burgunder, F. Walker, A. M. Davis, M. Busse, L. Quinn, F. B. Rodrigues, C. Sampaio, C. G. Goetz, E. Cubo, P. Martinez-Martin, G. T. Stebbins; Members of the MDS Committee on Rating Scales Development, Quality of life in Huntington's disease: Critique and recommendations for measures assessing patient health-related quality of life and caregiver quality of life. *Mov. Disord.* **33**, 742–749 (2018).
9. S. J. Tabrizi, D. R. Langbehn, B. R. Leavitt, R. A. Roos, A. Durr, D. Craufurd, C. Kennard, S. L. Hicks, N. C. Fox, R. I. Scahill, B. Borowsky, A. J. Tobin, H. D. Rosas, H. Johnson, R. Reilmann, B. Landwehrmeyer, J. C. Stout; TRACK-HD investigators, Biological and clinical manifestations of Huntington's disease in the longitudinal TRACK-HD study: Cross-sectional analysis of baseline data. *Lancet Neurol.* **8**, 791–801 (2009).
10. S. J. Tabrizi, R. Reilmann, R. A. C. Roos, A. Durr, B. Leavitt, G. Owen, R. Jones, H. Johnson, D. Craufurd, S. L. Hicks, C. Kennard, B. Landwehrmeyer, J. C. Stout, B. Borowsky, R. I. Scahill, C. Frost, D. R. Langbehn; TRACK-HD investigators, Potential endpoints for clinical trials in premanifest and early Huntington's disease in the TRACK-HD study: Analysis of 24 month observational data. *Lancet Neurol.* **11**, 42–53 (2012).
11. S. J. Tabrizi, R. I. Scahill, G. Owen, A. Durr, B. R. Leavitt, R. A. Roos, B. Borowsky, B. Landwehrmeyer, C. Frost, H. Johnson, D. Craufurd, R. Reilmann, J. C. Stout, D. R. Langbehn; TRACK-HD Investigators, Predictors of phenotypic progression and disease onset in premanifest and early-stage Huntington's disease in the TRACK-HD study: Analysis of 36-month observational data. *Lancet Neurol.* **12**, 637–649 (2013).
12. L. M. Byrne, E. J. Wild, Cerebrospinal fluid biomarkers for Huntington's disease. *J. Huntingtons Dis.* **5**, 1–13 (2016).
13. E. J. Wild, R. Boggio, D. Langbehn, N. Robertson, S. Haider, J. R. C. Miller, H. Zetterberg, B. R. Leavitt, R. Kuhn, S. J. Tabrizi, D. Macdonald, A. Weiss, Quantification of mutant huntingtin protein in cerebrospinal fluid from Huntington's disease patients. *J. Clin. Invest.* **125**, 1979–1986 (2015).
14. Ionis Pharmaceuticals, Ionis Pharmaceuticals Licenses IONIS-HTT Rx to partner following successful phase 1/2a study in patients with Huntington's disease (2017); http://ir.ionispharma.com/news-releases/news-release-details/ionis-pharmaceuticals-licenses-ionis-htt-rx-partner-following.
15. V. Fodale, R. Boggio, M. Daldin, C. Cariulo, M. C. Spiezia, L. M. Byrne, B. R. Leavitt, E. J. Wild, D. Macdonald, A. Weiss, A. Bresciani, Validation of ultrasensitive mutant huntingtin detection in human cerebrospinal fluid by single molecule counting immunoassay. *J. Huntingtons Dis.* **6**, 349–361 (2017).
16. P. N. Hoffman, R. J. Lasek, The slow component of axonal transport. Identification of major structural polypeptides of the axon and their generality among mammalian neurons. *J. Cell Biol.* **66**, 351–366 (1975).
17. P. Shahim, Y. Tegner, B. Gustafsson, M. Gren, J. Ärlig, M. Olsson, N. Lehto, Å. Engström, K. Höglund, E. Portelius, H. Zetterberg, K. Blennow, Neurochemical aftermath of repetitive mild traumatic brain injury. *JAMA Neurol.* **73**, 1308–1315 (2016).
18. R. Constantinescu, M. Romer, D. Oakes, L. Rosengren, K. Kieburtz, Levels of the light subunit of neurofilament triplet protein in cerebrospinal fluid in Huntington's disease. *Parkinsonism Relat. Disord.* **15**, 245–248 (2009).
19. T. Vinther-Jensen, L. Börnsen, E. Budtz-Jørgensen, C. Ammitzbøll, I. U. Larsen, L. E. Hjermind, F. Sellebjerg, J. E. Nielsen, Selected CSF biomarkers indicate no evidence of early neuroinflammation in Huntington disease. *Neurol. Neuroimmunol. Neuroinflamm.* **3**, e287 (2016).
20. V. Niemelä, A.-M. Landtblom, K. Blennow, J. Sundblom, Tau or neurofilament light—Which is the more suitable biomarker for Huntington's disease? *PLOS ONE* **12**, e0172762 (2017).
21. F. B. Rodrigues, L. M. Byrne, P. McColgan, N. Robertson, S. J. Tabrizi, H. Zetterberg, E. J. Wild, Cerebrospinal fluid inflammatory biomarkers reflect clinical severity in Huntington's disease. *PLOS ONE* **11**, e0163479 (2016).
22. L. M. Byrne, F. B. Rodrigues, K. Blennow, A. Durr, B. R. Leavitt, R. A. C. Roos, R. I. Scahill, S. J. Tabrizi, H. Zetterberg, D. Langbehn, E. J. Wild, Neurofilament light protein in blood as a potential biomarker of neurodegeneration in Huntington's disease: A retrospective cohort analysis. *Lancet Neurol.* **16**, 601–609 (2017).
23. E. B. Johnson, L. M. Byrne, S. Gregory, F. B. Rodrigues, K. Blennow, A. Durr, B. R. Leavitt, R. A. Roos, H. Zetterberg, S. J. Tabrizi, R. I. Scahill, E. J. Wild; TRACK-HD Study Group, Neurofilament light protein in blood predicts regional atrophy in Huntington disease. *Neurology* **90**, e717–e723 (2018).
24. R. Soylu-Kucharz, Å. Sandelius, M. Sjögren, K. Blennow, E. J. Wild, H. Zetterberg, M. Björkqvist, Neurofilament light protein in CSF and blood is associated with neurodegeneration and disease severity in Huntington's disease R6/2 mice. *Sci. Rep.* **7**, 14114 (2017).

25. H. M. Fonteijn, M. Modat, M. J. Clarkson, J. Barnes, M. Lehmann, N. Z. Hobbs, R. I. Scahill, S. J. Tabrizi, S. Ourselin, N. C. Fox, D. C. Alexander, An event-based model for disease progression and its application in familial Alzheimer's disease and Huntington's disease. *Neuroimage* **60**, 1880–1889 (2012).
26. B. M. Young, Z. Nigogosyan, L. M. Walton, J. Song, V. A. Nair, S. W. Grogan, M. E. Tyler, D. F. Edwards, K. Caldera, J. A. Sattin, J. C. Williams, V. Prabhakaran, Changes in functional brain organization and behavioral correlations after rehabilitative therapy using a brain-computer interface. *Front. Neuroeng.* **7**, 26 (2014).
27. N. P. Oxtoby, A. L. Young, D. M. Cash, T. L. S. Benzinger, A. M. Fagan, J. C. Morris, R. J. Bateman, N. C. Fox, J. M. Schott, D. C. Alexander, Data-driven models of dominantly-inherited Alzheimer's disease progression. *Brain* **141**, 1529–1544 (2018).
28. A. L. Young, N. P. Oxtoby, P. Daga, D. M. Cash, N. Fox, S. Ourselin, J. M. Schott, D. C. Alexander, A data-driven model of biomarker changes in sporadic Alzheimer's disease. *Alzheimers Dement.* **10**, P172 (2014).
29. A. Eshaghi, R. V. Marinescu, A. L. Young, N. C. Firth, F. Prados, M. J. Cardoso, C. Tur, F. De Angelis, N. Cawley, W. Brownlee, N. De Stefano, M. L. Stromillo, M. Battaglini, S. Ruggieri, C. Gasperini, M. Filippi, M. A. Rocca, A. Rovira, J. Sastre-Garriga, J. Geurts, H. Vrenken, V. Wottschel, C. E. Leurs, B. Uitdehaag, L. Pirpamer, C. Enzinger, S. Ourselin, C. A. G. Wheeler-Kingshott, D. Chard, A. J. Thompson, F. Barkhof, D. C. Alexander, O. Ciccarelli, Progression of regional grey matter atrophy in multiple sclerosis. *Brain* **141**, 1665–1677 (2017).
30. P. A. Wijeratne, A. L. Young, N. P. Oxtoby, R. V. Marinescu, N. C. Firth, E. B. Johnson, A. Mohan, C. Sampaio, R. I. Scahill, S. J. Tabrizi, D. C. Alexander, An image-based model of brain volume biomarker changes in Huntington's disease. *Ann. Clin. Transl. Neurol.* **5**, 570–582 (2018).
31. L. B. Lusted, Signal detectability and medical decision-making. *Science* **171**, 1217–1219 (1971).
32. J. D. Long, J. A. Mills, B. R. Leavitt, A. Durr, R. A. Roos, J. C. Stout, R. Reilmann, B. Landwehrmeyer, S. Gregory, R. I. Scahill, D. R. Langbehn, S. J. Tabrizi; Track-HD and Track-On Investigators, Survival end points for Huntington disease trials prior to a motor diagnosis. *JAMA Neurol.* **74**, 1352–1360 (2017).
33. A. L. Southwell, S. E. P. Smith, T. R. Davis, N. S. Caron, E. B. Villanueva, Y. Xie, J. A. Collins, M. Li Ye, A. Sturrock, B. R. Leavitt, A. G. Schrum, M. R. Hayden, Ultrasensitive measurement of huntingtin protein in cerebrospinal fluid demonstrates increase with Huntington disease stage and decrease following brain huntingtin suppression. *Sci. Rep.* **5**, 12166 (2015).
34. D. J. Hensman Moss, A. F. Pardiñas, D. Langbehn, K. Lo, B. R. Leavitt, R. Roos, A. Durr, S. Mead; TRACK-HD investigators, REGISTRY investigators, P. Holmans, L. Jones, S. J. Tabrizi, Identification of genetic variants associated with Huntington's disease progression: A genome-wide association study. *Lancet Neurol.* **16**, 701–711 (2017).
35. Genetic Modifiers of Huntington's Disease (GeM-HD) Consortium, Identification of genetic factors that modify clinical onset of Huntington's disease. *Cell* **162**, 516–526 (2015).
36. G. Bates, S. J. Tabrizi, L. Jones, *Huntington's Disease* (Oxford Univ. Press, ed. 4, 2014).
37. P. Shahim, M. Gren, V. Liman, U. Andreasson, N. Norgren, Y. Tegner, N. Mattsson, N. Andreasen, M. Öst, H. Zetterberg, B. Nellgård, K. Blennow, Serum neurofilament light protein predicts clinical outcome in traumatic brain injury. *Sci. Rep.* **6**, 36791 (2016).
38. P. Shahim, Y. Tegner, D. H. Wilson, J. Randall, T. Skillbäck, D. Pazooki, B. Kallberg, K. Blennow, H. Zetterberg, Blood biomarkers for brain injury in concussed professional ice hockey players. *JAMA Neurol.* **71**, 684–692 (2014).
39. G. Disanto, C. Barro, P. Benkert, Y. Naegelin, S. Schädelin, A. Giardiello, C. Zecca, K. Blennow, H. Zetterberg, D. Leppert, L. Kappos, C. Gobbi, J. Kuhle; Swiss Multiple Sclerosis Cohort Study Group, Serum neurofilament light: A biomarker of neuronal damage in multiple sclerosis. *Ann. Neurol.* **81**, 857–870 (2017).
40. L. Novakova, H. Zetterberg, P. Sundström, M. Axelsson, M. Khademi, M. Gunnarsson, C. Malmeström, A. Svenningsson, T. Olsson, F. Piehl, K. Blennow, J. Lycke, Monitoring disease activity in multiple sclerosis using serum neurofilament light protein. *Neurology* **89**, 2230–2237 (2017).
41. O. Y. Glushakova, A. V. Glushakov, E. R. Miller, A. B. Valadka, R. L. Hayes, Biomarkers for acute diagnosis and management of stroke in neurointensive care units. *Brain Circ.* **2**, 28–47 (2016).
42. F. Al Nimer, E. Thelin, H. Nyström, A. M. Dring, A. Svenningsson, F. Piehl, D. W. Nelson, B.-M. Bellander, Comparative assessment of the prognostic value of biomarkers in traumatic brain injury reveals an independent role for serum levels of neurofilament light. *PLOS ONE* **10**, e0132177 (2015).
43. M. Gisslén, R. W. Price, U. Andreasson, N. Norgren, S. Nilsson, L. Hagberg, D. Fuchs, S. Spudich, K. Blennow, H. Zetterberg, Plasma concentration of the neurofilament light protein (NFL) is a biomarker of CNS injury in HIV infection: A cross-sectional study. *EBioMedicine* **3**, 135–140 (2015).
44. J. D. Rohrer, I. O. C. Woollacott, K. M. Dick, E. Brotherhood, E. Gordon, A. Fellows, J. Toombs, R. Druyeh, M. J. Cardoso, S. Ourselin, J. M. Nicholas, N. Norgren, S. Mead, U. Andreasson, K. Blennow, J. M. Schott, N. C. Fox, J. D. Warren, H. Zetterberg, Serum neurofilament light chain protein is a measure of disease intensity in frontotemporal dementia. *Neurology* **87**, 1329–1336 (2016).
45. O. Hansson, S. Janelidze, S. Hall, N. Magdalinou, A. J. Lees, U. Andreasson, N. Norgren, J. Linder, L. Forsgren, R. Constantinescu, H. Zetterberg, K. Blennow; Swedish BioFINDER study, Blood-based NfL: A biomarker for differential diagnosis of parkinsonian disorder. *Neurology* **88**, 930–937 (2017).
46. P. Shahim, H. Zetterberg, Y. Tegner, K. Blennow, Serum neurofilament light as a biomarker for mild traumatic brain injury in contact sports. *Neurology* **88**, 1788–1794 (2017).
47. J. S. Paulsen, M. Hayden, J. C. Stout, D. R. Langbehn, E. Aylward, C. A. Ross, M. Guttman, M. Nance, K. Kieburtz, D. Oakes, I. Shoulson, E. Kayson, S. Johnson, E. Penziner; Predict-HD Investigators of the Huntington Study Group, Preparing for preventive clinical trials: The Predict-HD study. *Arch. Neurol.* **63**, 883–890 (2006).
48. L. M. Byrne, F. B. Rodrigues, E. B. Johnson, E. De Vita, K. Blennow, R. Scahill, H. Zetterberg, A. Heslegrave, E. J. Wild, Cerebrospinal fluid neurogranin and TREM2 in Huntington's disease. *Sci. Rep.* **8**, 4260 (2018).
49. CHDI Foundation, About This Study | Enroll-HD; www.enroll-hd.org/learn/about-this-study/.
50. J. G. Sled, A. P. Zijdenbos, A. C. Evans, A nonparametric method for automatic correction of intensity nonuniformity in MRI data. *IEEE Trans. Med. Imaging* **17**, 87–97 (1998).
51. P. A. Freeborough, N. C. Fox, R. I. Kitney, Interactive algorithms for the segmentation and quantitation of 3-D MRI brain scans. *Comput. Methods Programs Biomed.* **53**, 15–25 (1997).
52. J. L. Whitwell, W. R. Crum, H. C. Watt, N. C. Fox, Normalization of cerebral volumes by use of intracranial volume: Implications for longitudinal quantitative MR imaging. *AJNR Am. J. Neuroradiol.* **22**, 1483–1489 (2001).
53. R. I. Scahill, C. Frost, R. Jenkins, J. L. Whitwell, M. N. Rossor, N. C. Fox, A longitudinal study of brain volume changes in normal aging using serial registered magnetic resonance imaging. *Arch. Neurol.* **60**, 989–994 (2003).
54. J. Ashburner, K. J. Friston, Voxel-based morphometry—The methods. *Neuroimage* **11**, 805–821 (2000).
55. C. Ledig, R. A. Heckemann, A. Hammers, J. C. Lopez, V. F. J. Newcombe, A. Makropoulos, J. Lötjönen, D. K. Menon, D. Rueckert, Robust whole-brain segmentation: Application to traumatic brain injury. *Med. Image Anal.* **21**, 40–58 (2015).
56. E. B. Johnson, S. Gregory, H. J. Johnson, A. Durr, B. R. Leavitt, R. A. Roos, G. Rees, S. J. Tabrizi, R. I. Scahill, Recommendations for the use of automated gray matter segmentation tools: Evidence from Huntington's disease. *Front. Neurol.* **8**, 519 (2017).
57. E. R. DeLong, D. M. DeLong, D. L. Clarke-Pearson, Comparing the areas under two or more correlated receiver operating characteristic curves: A nonparametric approach. *Biometrics* **44**, 837–845 (1988).

Acknowledgments: We would like to thank all the participants from the HD community who donated samples and gave their time to take part in this study. **Funding:** This work was supported by the Medical Research Council UK (Clinician Scientist Fellowship MR/M008592/1), CHDI Foundation, the Wellcome Trust [Wellcome Collaborative Award In Science 200181/Z/15/Z and Wellcome/Engineering and Physical Sciences Research Council Centre for Medical Engineering (WT 203148/Z/16/Z)], the Department of Health's National Institute for Health Research Biomedical Research Centres funding scheme, the UK Dementia Research Institute, Hoffman La Roche, Horizon 2020 Framework Programme, and Engineering and Physical Sciences Research Council. **Author contributions:** H.Z., R.I.S., D.C.A., and E.J.W. designed the study. L.M.B. and F.B.R. contributed to participant recruitment and sample collection. L.M.B., F.B.R., E.B.J., and E.D.V. were involved in acquiring data. E.D.V. optimized MRI protocol. E.B.J. and R.I.S. performed MRI processing. A.H. processed patient samples. P.A.W. developed and performed the EBM analysis. G.P. performed sample size calculations. L.M.B. and F.B.R. performed the remaining statistical analysis. L.M.B., F.B.R., and E.J.W. interpreted data and wrote the manuscript. All authors contributed to reviewing the manuscript. **Competing interests:** Through UCL Consultants Ltd., a wholly owned subsidiary of University College London, E.J.W. has served on scientific advisory boards for Novartis, F. Hoffmann–La Roche, Ionis, Shire, Wave Life Sciences, PTC Therapeutics, and Mitoconix; and R.I.S. has undertaken consultancy services for Ixitech Ltd. H.Z. is a cofounder of Brain Biomarker Solutions, Gothenburg, Sweden; part of the holding company GU Ventures at the University of Gothenburg; and has served at advisory boards for Roche Diagnostics, Eli Lilly, and Wave. G.P., C.C., and S.S. are full-time employees of F. Hoffmann–LaRoche, and C.C. is also a stockholder. **Data and materials availability:** All data are included in the paper or in the Supplementary Materials.

Submitted 25 April 2018
Accepted 23 August 2018
Published 12 September 2018
10.1126/scitranslmed.aat7108

Citation: L. M. Byrne, F. B. Rodrigues, E. B. Johnson, P. A. Wijeratne, E. De Vita, D. C. Alexander, G. Palermo, C. Czech, S. Schobel, R. I. Scahill, A. Heslegrave, H. Zetterberg, E. J. Wild, Evaluation of mutant huntingtin and neurofilament proteins as potential markers in Huntington's disease. *Sci. Transl. Med.* **10**, eaat7108 (2018).

Science Translational Medicine

Evaluation of mutant huntingtin and neurofilament proteins as potential markers in Huntington's disease

Lauren M. Byrne, Filipe B. Rodrigues, Eileanor B. Johnson, Peter A. Wijeratne, Enrico De Vita, Daniel C. Alexander, Giuseppe Palermo, Christian Czech, Scott Schobel, Rachael I. Scahill, Amanda Heslegrave, Henrik Zetterberg and Edward J. Wild

Sci Transl Med **10**, eaat7108.
DOI: 10.1126/scitranslmed.aat7108

Improving Huntington's disease detection

Early detection of Huntington's disease (HD) could help the development of effective therapeutic strategies to block or delay disease progression. Byrne and colleagues now show that in blood and cerebrospinal fluid, mutant huntingtin (mHTT) and neurofilament light (NfL) protein concentrations correlated with disease severity in HD patients. Computational analysis further showed that alterations in circulating NfL and mHTT concentrations may be among the earliest detectable changes in HD. Thus, the results suggest that analysis of mHTT and NfL concentrations in biofluids might be used in combination with other clinical measures for improving the accuracy and efficiency of early HD detection.